Hydrogen−Deuterium (H/D) Exchange Mapping of Aβ_{1-40} Amyloid Fibril Secondary Structure Using Nuclear Magnetic Resonance Spectroscopy†

Neil A. Whittemore,‡,§ Rajesh Mishra,‡,§ Indu Kheterpal,|| Angela D. Williams,|| Ronald Wetzel,|| and Engin H. Serpersu*,§

Department of Biochemistry and Cellular and Molecular Biology, the Center of Excellence for Structural Biology, University of Tennessee−Knoxville, Knoxville, Tennessee 37996, and Graduate School of Medicine, University of Tennessee, Knoxville, Tennessee 37919

Received August 9, 2004; Revised Manuscript Received January 24, 2005

ABSTRACT: We describe here details of the hydrogen−deuterium (H/D) exchange behavior of the Alzheimer's peptide Aβ_{1-40}, while it is a resident in the amyloid fibril, as determined by high-resolution solution NMR. Kinetics of H/D exchange in Aβ_{1-40} fibrils show that about half the backbone amide protons exchange during the first 25 h, while the other half remain unexchanged because of solvent inaccessibility and/or hydrogen-bonded structure. After such a treatment for 25 h with D_2O, fibrils of ^{15}N-enriched Aβ were dissolved in a mixture of 95% dimethyl sulfoxide (DMSO) and 5% dichloroacetic acid (DCA) and successive heteronuclear ^{1}H-^{15}N HSQC spectra were collected to identify the backbone amides that did not exchange in the fibril. These studies showed that the N and C termini of the peptide are accessible to the solvent in the fibril state and the backbone amides of these residues are readily exchanged with bulk deuterium. In contrast, the residues in the middle of the peptide (residues 16−36) are mostly protected, suggesting that that many of the residues in this segment of the peptide are involved in a β structure in the fibril. Two residues, G25 and S26, exhibit readily exchangeable backbone amide protons and therefore may be located on a turn or a flexible part of the peptide. Overall, the data substantially supports current models for how the Aβ peptide folds when it engages in the amyloid fibril structure, while also addressing some discrepancies between models.

The structures of amyloid fibrils and related protein aggregates are currently of great interest. These aggregates are now recognized as constituting important alternative folded states of globular proteins and peptide fragments whose assembly processes and structures are providing new insights into the fundamental rules of protein folding. In addition, these alternative folding pathways are of significant biological consequence. It has been estimated that up to 50% of the polypeptide chains emerging from the ribosome do not mature into native, folded states but rather become degraded by mechanisms that recognize fatal misfolding steps that may otherwise lead to aggregation (*1*). The ability of some proteins to aggregate either inside or outside the cell has been linked to a wide variety of human diseases, including important neurodegenerative diseases (*2*).

Despite the importance of non-native protein aggregates such as the Aβ amyloid fibrils associated with Alzheimer's disease, progress toward the high-resolution structure analysis of aggregates using X-ray crystallography or solution-state multidimensional NMR spectroscopy has been slow and fraught with difficulties (*3*). However, key features of the peptide and protein conformations within the supramolecular architecture of Aβ amyloid fibrils have been revealed by a variety of techniques. X-ray fiber diffraction shows that many amyloid fibrils including Aβ fibrils possess a cross-β structure in which the β-extended chains are oriented perpendicular to the fibril axis, while the hydrogen bonds that connect these strands into β sheets are oriented parallel to the fibril axis (*4*). Limited proteolysis studies revealed that the N-terminal 10−15 residues of Aβ are not involved in the rigid, hydrogen-bonded core of amyloid fibrils (*5*). This result was supported by hydrogen−deuterium (H/D)[1] exchange studies, monitored by mass spectroscopy (MS), which showed that 50% of the 39 backbone amide hydrogens of Aβ_{1-40} are not involved in protective hydrogen bonds associated with a β sheet when this peptide is incorporated into the fibril structure (*6*, *7*). Although a antiparallel β sheet has been observed in some amyloid fibrils, including those derived from Aβ fragments (*8*), both solid-state NMR (*9*, *10*) and electron paramagnetic resonance (EPR) spectroscopy (*11*) show that Aβ_{1-40} amyloid fibrils contain a parallel β

† This research was supported by Grants MCB 01110741 from the National Science Foundation (to E.H.S.) and R01 AG18927 from the National Institutes of Health (to R.W. and E.H.S.).

* To whom correspondence should be addressed: Department of Biochemistry and Cellular and Molecular Biology, University of Tennessee−Knoxville, Walters Life Sciences Bldg. M407, Knoxville, TN 37996-0840. Telephone: 865-974-2668. Fax: 865-974-6306. E-mail: serpersu@utk.edu.

‡ These authors contributed equally to the work.

§ Department of Biochemistry and Cellular and Molecular Biology and the Center of Excellence for Structural Biology.

|| Graduate School of Medicine.

[1] Abbreviations: DMSO, dimethyl sulfoxide; DCA, dichloroacetic acid; HFIP, 1,1,1,3,3,3-hexafluoro-2-propanol; TFA, trifluoroacetic acid; HSQC, heteronuclear single-quantum coherence spectroscopy; TOCSY, total correlation spectroscopy; NOESY, nuclear Overhauser effect spectroscopy; H/D, hydrogen−deuterium.

10.1021/bi048292u CCC: $30.25
Published on Web 02/18/2005

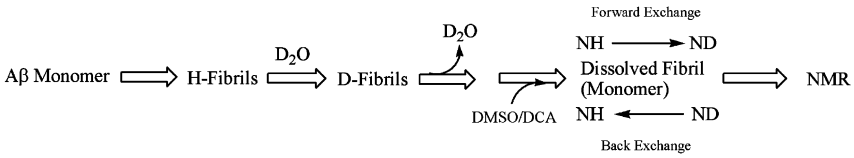

FIGURE 1: Schematic diagram summarizing the exchange experiment. Fibrils grown from protonated Aβ_{1-40} are exposed to a D_2O buffer allowing exchangeable protons to exchange with deuterium at rates controlled by the solvent exposure and hydrogen-bonding state of the protons. After removal of most of the D_2O, fibrils are brought up in DMSO/DCA, which dissolves the fibrils to monomers while minimizing further exchange with the residual H_2O/D_2O carried over with the fibrils from the aqueous exchange reaction. This solution is quickly analyzed to determine the H/D content of each identifiable backbone amide proton. In theory, this sample is susceptible during dissolution and analysis to both forward (with the deuterium component of the solvent) and back (with the hydrogen component of the solvent) exchange. These rates appear to be relatively small under these conditions, however, and are ignored in the analysis (see the text).

sheet in which residues on adjacent strands are in register within the hydrogen-bonded core of the fibril.

The next level of structure determination is how the Aβ chain folds on itself within the fibril. Conformational and proximity information is revealed directly in solid-state NMR spectra (*10*). Conformational flexibility can also be inferred by scanning proline mutagenesis linked to stability analysis (*12*). Portions of the Aβ peptide involved in hydrogen bonding within the fibril have been revealed by segmental H/D exchange protection analysis using proteolysis coupled with MS (*13*). These techniques broadly agree with the limited proteolysis data (*5*) in suggesting an exposed and flexible N terminus and also agree with each other in indicating two major segments of a rigid β structure. There are also a number of differences among models derived from these various approaches, such as whether the extreme C terminus of Aβ_{1-40} is or is not involved in an extended β-sheet structure, indicating that further studies are in order.

Single-residue resolution protection factors from H/D experiments would greatly contribute to our knowledge of the exact folding pattern of the Aβ peptide within the fibril structure. H/D exchange monitored by NMR has been used for decades to identify backbone amide protons involved in protective secondary structure within globular proteins at single-residue resolution (*14*, *15*). More recently, several groups have described H/D NMR experiments on amyloid fibrils synthesized from β-2 microglobulin, transthyretin, and fragments of the Aβ peptide (residues 25−35) and prion protein (*16*−*19*). Here, we describe the application of similar techniques to the analysis of amyloid fibrils of full-length Aβ_{1-40} to reveal those residues involved in highly protective hydrogen-bonded structure (*20*). The data are broadly consistent with models of the Aβ fibril derived from the experimental approaches listed above. At the same time, the data address previously reported differences, in particular, the position of turns within the Aβ peptide and the status of various sequence elements in the C-terminal portion of the molecule.

MATERIALS AND METHODS

Materials. Shigemi NMR tubes (Shigemi, Inc., Allison Park, PA) that were matched to DMSO-d_6 were used in all of the experiments. DMSO-d_6 and D_2O were obtained from Cambridge Isotope Laboratories (Andover, MA), and dichloroacetic acid-d_2 (DCA) was purchased from Aldrich Chemical Co. (Milwaukee, WI). 1,1,1,3,3,3-Hexafluoro-2-propanol (HFIP) was obtained from Acros Organics (Morris Planes, NJ), and trifluoroacetic acid (TFA) was purchased from Pierce (Rockford, IL). Chemically synthesized Aβ_{1-40} peptide was obtained from the Keck Biotechnology Center (Yale University, New Haven, CT), and the recombinantly prepared *U*-^{15}N Aβ_{1-40} peptide was obtained from rPeptide (Athens, GA).

Synthesis and H/D Exchange of Aβ_{1-40} and Fibrils. A typical fibril preparation was performed as previously described in detail (*5*, *6*). Briefly, Aβ_{1-40} or *U*-^{15}N-enriched Aβ_{1-40} peptide was treated with TFA and HFIP to remove any pre-existing aggregates, lyophilized, and then dissolved in 2 mM NaOH and 2× PBS (20 mM phosphate, 276 mM sodium chloride, and 5.4 mM KCl containing 0.1% sodium azide at pH 7.4) in an equal volume ratio. Fibril formation was started by the addition of sonicated fibrils [1:1000 (w/w)] from a previous fibril preparation followed by incubation of these solutions at 37 °C for 5−7 days. Fibril growth was monitored by thioflavin T fluorescence, and the quality of the fibrils was monitored by electron microscopy.

For H/D exchange experiments, fibrils were isolated by centrifugation at 13000*g* for 30 min, resuspended with a gentle vortex in D_2O, and incubated for 25 h at room temperature in 2.5 mM deuterated Tris-HCl buffer at pH 7.5. This time was selected based on H/D exchange kinetics of Aβ_{1-40} fibrils monitored by MS, which show that exchange of backbone amide hydrogens with deuteriums is relatively slow after 24 h (*6*). After the D_2O treatment, fibrils were again collected by centrifugation and were carefully dried using strips of filter paper to wick off the residual D_2O. Fibrils were then dissolved in 250 μL of 95% DMSO/5% DCA (DMSO/DCA) mixture under nitrogen and immediately transferred to Shigemi NMR tube to start the data acquisition. The time from the start of fibril dissolution to the start of NMR experiments was 14 min. Concentration of the peptide was checked by HPLC after NMR experiments. Upon the completion of this series of experiments, 35 μL of deionized water was added to the Shigemi tube and was used to acquire data for the fully protonated dissolved monomer peptide (separate control experiments showed that the spectra were identical to the spectrum of the fibril dissolved in the same solvent mixture without the D_2O treatment).

A schematic representation of the experimental strategy for the H/D exchange in the fibril state and after the dissolution of fibril is shown in Figure 1. In this context, the "dissolved fibril" indicates the Aβ_{1-40} peptide obtained by dissolution of the fibrils in the DMSO/DCA mixture. The term forward exchange is used to indicate the continued exchange of amide protons with deuterium after the dissolution of fibrils in DMSO/DCA. The back exchange refers to reprotonation of already exchanged amides because of solvent composition in the dissolved fibrils.

NMR Spectroscopy. For the NMR studies of the wild-type (WT) Aβ_{1-40} monomer and solution after dissolving the fibrils in DMSO/DCA, 250 μL solutions (70−180 μM in equivalent monomer concentration) were placed in a Shigemi NMR tube. The transfer of the solution to the Shigemi NMR tube was performed under an inert atmosphere of dry nitrogen in a polyethylene glovebag (Aldrich Chemical Co., Milwaukee, WI). NMR experiments were performed on a 600 MHz Varian INOVA (Varian, Inc., Palo Alto, CA) instrument that was equipped with a single gradient axis and a triple resonance probe for the observation of proton, carbon, and nitrogen nuclei. Two-dimensional NMR data were acquired in phase-sensitive mode using the States−Haberkorn method for quadrature detection in the indirect dimension (*21*). The residual water was saturated with low power before data acquisition. The DMSO peak was referenced as 2.49 ppm in all spectra. Two-dimensional homonuclear nuclear Overhauser effect spectroscopy (NOESY) (*22*) spectra were recorded with mixing times of 75, 100, 150, and 200 ms. Total correlation spectroscopy (TOCSY) (*23*) spectra were recorded using the decoupling in the presence of scalar interaction (DIPSI) spin-lock sequence with a 8 kHz RF field and mixing times of 25 and 60 ms. Typically, spectra were acquired with 256 t_1 increments, 2048 data points, a relaxation delay of 1 s, and a spectral width of 8500 Hz. Spectra were recorded with 64 scans per increment for NOESY and 32 scans per increment for TOCSY. In all NOESY and TOCSY spectra, the data are multiplied by a 60−90° phase shifted $\sin^2$ window function in both dimensions before Fourier transformation.

A 250 μL sample of *U*-^{15}N-enriched Aβ_{1-40} fibrils dissolved in DMSO/DCA (500 μM in monomer concentration) was used to determine the extent of H/D exchange in fibrils treated with D_2O. A sensitivity enhanced ^{1}H-^{15}N heteronuclear single-quantum coherence spectroscopy (HSQC) spectrum (*24*), from the BioPack set of pulse sequences for the Varian spectrometer, was acquired from the solution of dissolved monomeric peptide in the phase-sensitive mode using the States−Haberkorn method for quadrature detection in the indirect dimension (*21*). The dataset is obtained with a spectral width of 10 000 Hz in the ^{1}H dimension and 2127.55 Hz in the ^{15}N dimension, and 56 scans of 640 real-time points for each of 128 t_1 increments were recorded for approximately 33.5 min. The data are processed using the Felix processing software package. The ^{1}H dimension was zero-filled to 1024 points with the sensitivity enhancement option selected on the left half of the spectrum (effective sweep width of 5000 Hz). The center frequency of the spectrum in each dimension was referenced according to the υ_0 ^{1}H and υ_0 ^{15}N that was determined using a sample of 2,2-dimethyl-2-silapentane-5-sulfonate sodium salt (DSS) in DMSO/DCA, 2.51 ppm for the 1024 point and 116 ppm for the 64 point, for ^{1}H and ^{15}N dimension, respectively (*25*). Critical in assignment of the ^{15}N resonances was the acquisition of 3D HNHA and HNHB (*26*) spectra. Both experiments were acquired in the same phase-sensitive manner: spectral widths of ^{1}H, ^{1}H, and ^{15}N were 8000, 6400, and 1800 Hz, respectively, with 16 scans of 512 real-time points for each of the 32 and 16 t_1 and t_2 increments, respectively. These spectra also aided in the assignments of the N-H fingerprint region.

Processing and Analysis of the Data. All data are processed using the Felix software (Accelrys, Carlsbad, CA). Analysis for the assignment of the ^{1}H resonances was performed using Sparky (Tom Goddard, UCSF, San Francisco, CA). In the H/D exchange studies, the *Assign* module of Felix was used to assign the ^{15}N resonances. The volume of the peaks in the HSQC spectra was measured by using the Felix software package.

RESULTS

Selection of a Suitable Solvent for H/D Exchange Mapping Studies. The nature of the experiments described here is to determine the amount of H/D exchange that has occurred at each exchangeable position in the peptide, when the peptide is resident in the fibril. However, amyloid fibrils are not amenable for high-resolution, solution-phase NMR studies. Thus, to obtain interpretable NMR spectra allowing an evaluation of the degree of deuterium incorporation, it is necessary to perform the analysis indirectly on the dissolved monomeric peptide obtained by dissolution of fibrils in a suitable solvent (*16*−*19*, *27*) (for a cartoon of the approach, refer to Figure 1). The H/D exchange map of the original Aβ_{1-40} amyloid fibril is obtained indirectly from the H/D exchange characteristics of the soluble monomer after dissolving the deuterated amyloid fibril in an appropriate solvent. To obtain an accurate H/D exchange map of the amyloid fibril once the fibrils are dissolved, the continued exchange of protons/deuterons between the dissolved fibril and the bulk solvent should be either eliminated or significantly reduced. In Figure 1, the two modes of H/D exchange after the dissolution of the fibril are shown, forward and back exchange. Forward exchange is the transfer of a deuteron from the bulk solvent (or another molecule of monomer) to an amide or amino proton. Conversely, the term back exchange is the transfer of a proton from the bulk solvent or other molecule of monomer to an amide or amino deuteron. The optimal solvent for H/D mapping of the amyloid fibril is one that efficiently dissolves the fibrils to their monomer units, suppresses as much as possible the forward- and back-exchange reactions that occur after fibrils have been dissolved, and promotes good dispersion of the NMR signals in the appropriate region of interest in the NMR spectrum. A solvent completely lacking exchangeable protons is ideal, because that should completely inhibit back exchange with the solvent. However, in practical terms, because water cannot be completely excluded when fibrils are dissolved in polar, aprotic solvents, some solvent water contamination is likely to be observed.

DMSO is shown to be an excellent solvent for H/D exchange studies of different amyloid fibrils, because it has no exchangeable protons and different types of amyloid fibrils easily dissolve in solutions with a high percentage of DMSO (*16*−*18*, *28*). Our initial efforts focused on dissolving the Aβ_{1-40} fibrils in pure DMSO. However, unlike amyloid fibrils generated from a fragment of Aβ_{1-40} (*17*), fibrils of full-length Aβ_{1-40} did not dissolve in neat DMSO. The presence of dichloroacetic acid (DCA) was necessary to dissolve the fibrils. DCA and other solvents in DMSO have been used to dissolve various fibrils for H/D exchange studies by NMR (*16*, *18*, *27*). A mixture of 2% DCA in DMSO solution was capable of dissolving the Aβ_{1-40} fibrils within several minutes; however, for complete dissolution of fibrils

within a few seconds, it is necessary to use 5% DCA in DMSO. In these solvent trials, complete dissolution of the fibrils to soluble monomers (dissolved Aβ_{1-40} fibrils) was confirmed by thioflavin assay, HPLC, and ultracentrifugation. Additionally, observation of sharp peaks in the NMR spectra confirmed that the original Aβ_{1-40} fibrils had been converted to small molecular weight species. Close examination of the NOESY and TOCSY spectra of the freshly dissolved Aβ_{1-40} monomer in this solvent mix showed the same spectral pattern as the dissolved Aβ_{1-40} fibrils, with only small differences in the intensities of some of the side-chain NOEs. Therefore, this mixture of 95% DMSO and 5% DCA was selected as a suitable mixture and will be referred to as DMSO/DCA.

2D NMR Spectroscopy of the Dissolved Aβ_{1-40} Fibrils. Initial studies were performed with fibrils that were formed from the WT Aβ_{1-40} monomer. Two-dimensional NMR spectra, acquired of such fibrils dissolved in DMSO/DCA, showed that there is a reasonable dispersion in the fingerprint region that shows the intraresidue and sequential NH-Hα correlations of both spectra, which allowed the assignments of the backbone resonances of all but V40 to be made based on standard scalar and NOE connectivity analysis (*29*, *30*) (Table S1 in the Supporting Information). The NH-Hα regions of TOCSY and NOESY spectra are shown in Figure 2 with several of the assignments marked. There were a number of sequential NH_i-NH_{i+1} NOE cross-peaks in the NOESY spectrum of the dissolved monomeric peptide. Especially, the stretch spanning residues 16−24 showed continuous NH_i-NH_{i+1} NOEs. This suggests that, although completely exposed to the solvent, this section of the peptide in DMSO/DCA may form an open loop, or the peptide may have an overall structure containing several turns. We do not know the significance of this observation to the conformation of Aβ_{1-40} in fibrils, but it is interesting to note that Mikros et al. (*31*) also observed consecutive NH_i-NH_{i+1} NOEs between residues 9 and 26 in HR-MAS studies of intact Aβ_{1-28} fibrils. Another plausible explanation for the observation of these NOEs is the presence of helical regions, which was previously reported by Craik and co-workers for Aβ_{1-40} in a water−micelle environment (*32*). This is however less likely in our conditions, and no $\alpha N_{i,i+3}$ NOEs were observed to support this possibility. In any case, the nature of the conformation of Aβ in the analysis buffer is only a technical issue within the context of this paper. Because the hydrogen exchange information of interest is what is established when Aβ fibrils are exposed to exchange in native buffer, any possible conformations of the Aβ monomer in the DMSO/DCA analysis buffer do not influence the critical structural interpretations of the data. Likewise, Aβ monomer conformation in DMSO/DCA does not have any implications for the conformation of the peptide in the aqueous phase in native buffer.

For reasons detailed in the following section, *U*-^{15}N-enriched fibrils were required for the H/D exchange mapping study. The ^{1}H-^{15}N HSQC spectrum of these fully protonated, dissolved Aβ_{1-40} fibrils revealed that the complete assignments of the N-H (amide) cross-peaks would require additional data. Therefore, 3D HNHA and HNHB experiments were also performed with this sample to aid in resonance assignments (*26*). Despite the availability of 3D HNHA and HNHB spectra, a few assignments still remained tentative

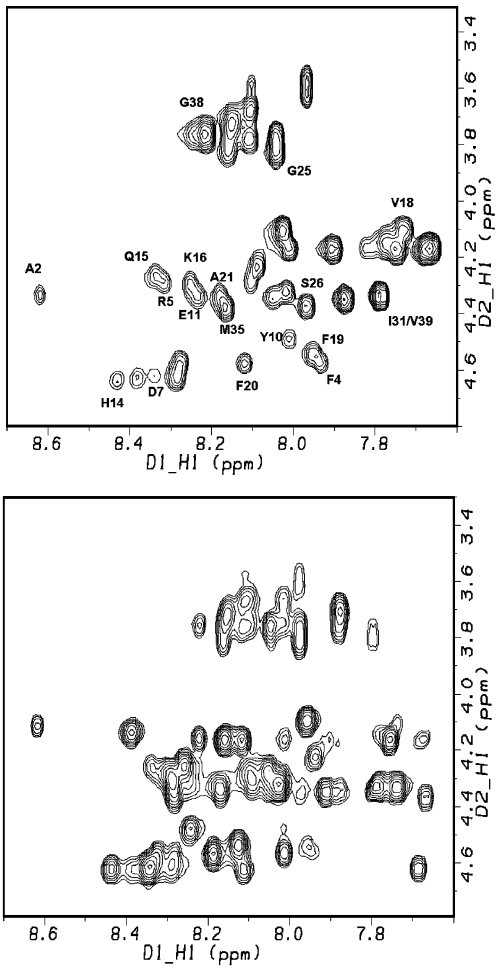

FIGURE 2: Fingerprint regions of TOCSY (top) and NOESY (bottom) spectra, acquired with fibrils of Aβ_{1-40} dissolved in 95% DMSO/5% DCA (DMSO/DCA) with a mixing time of 60 and 150 ms, respectively. Several NH-Hα assignments are shown in the TOCSY spectrum.

(V24, V36, and V40, Table S1 in the Supporting Information). Nevertheless, most of the assignments were made, and the cross-peaks in ^{1}H-^{15}N HSQC spectra allowed identification of the residues with protected backbone amides in fibrils.

H/D Exchange Mapping of the Aβ_{1-40} Fibrils. One- and two-dimensional NMR experiments revealed that when the WT Aβ_{1-40} fibrils are dissolved in DMSO-d_6/DCA-d_2 mixture the amide protons of the dissolved monomers exchange almost completely with the bulk deuterium within 120 min after dissolution. Therefore, data must be collected rapidly, necessitating H/D exchange experiments on *U*-^{15}N-enriched Aβ_{1-40} fibrils. The *U*-^{15}N-enriched fibrils were prepared as the WT Aβ_{1-40} fibrils used in this study. Electron micrographs confirmed that the structure of the *U*-^{15}N-enriched fibrils was similar to the WT fibrils (Figure S1 in the Supporting Information). The *U*-^{15}N-enriched fibrils were treated for 25 h in a 2.4 mM Tris-HCl deuterated buffer at pH 7.5 as described in the previous work from our group, and the 25 h sampling point was selected based on data from the same H/D MS study (Figure 3) (*6*). As shown in Figure 3, amides with fast and intermediary exchange rates are completely exchanged and only the protected core amides remained protonated at this time point. Therefore, the fibrils were treated with D_2O for a 25 h period and then a series of ^{1}H-^{15}N HSQC spectra were collected in succession to

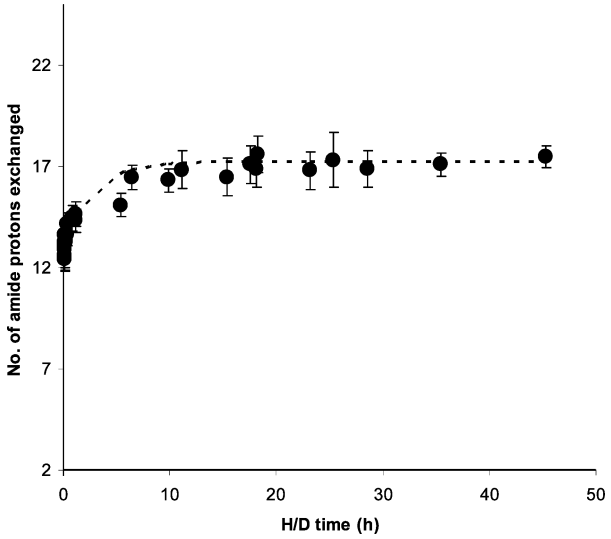

FIGURE 3: Number of amide protons exchanged versus the H/D exchange time in Aβ_{1-40} fibrils incubated in a 2.5 mM deuterated Tris-HCl buffer at pH 7.5. Data are similar to what has been previously published (*6*), except here it has been corrected for forward and back exchange.

determine not only the identity of the protected amide protons in fibrils exposed to treatment with deuterated Tris-HCl buffer but also to monitor their forward and back exchange rates in DMSO-d_6/DCA-d_2 mixture after the dissolution of the fibrils.

Figure 4 shows three ^{1}H-^{15}N HSQC spectra, acquired with dissolved Aβ_{1-40} fibrils in DMSO-d_6/DCA-d_2. Figure 4A is the fully protonated spectrum shown with some of the resonance assignments, and Figure 4B represents the first spectrum acquired after dissolution of the fibrils (data acquisition started 14 min after dissolution). Figure 4C shows the spectrum of the same sample in Figure 4B after ~3 h. Scrutiny of these spectra indicates that all of the amide proton chemical shifts are within a 1 ppm range and ^{15}N chemical shifts for all glycines and serines are more upfield than the rest, which indicates that the Aβ_{1-40} monomer is unfolded under these conditions. The first spectrum acquired after the exchange (Figure 4B) shows that some of the amide protons and all of the exchangeable side-chain protons are already exchanged with bulk deuterium. Some of the amide protons, however, are still strongly present in this spectrum.

The percent protection of the each residue compared to the intensity of the corresponding signal observed under fully protonated conditions is determined by the ratio of their intensity. The intensities are determined by integration of the volume of the spectral signals. The results are shown as a bar plot in Figure 5. In this plot, no volumes for residues V24, V36, and V40 are shown because of overlap and ambiguity in their N-H cross-peak assignments. Also, the apparent ~10% protection observed with several residues represent the final H/D ratio in the solvent mixture and not a fractional protection for these residues. This plot highlights a few significant features of the structure of Aβ_{1-40} fibrils. The first noticeable feature of the plot is that the N and C termini of Aβ_{1-40} in fibrils have more exchangeable protons than the central portion of the peptide. Also, the amide protons of residues 16−23 represent the most protected region of the peptide in fibrils; the only exception in this region is the low protection of A21. Another feature of the

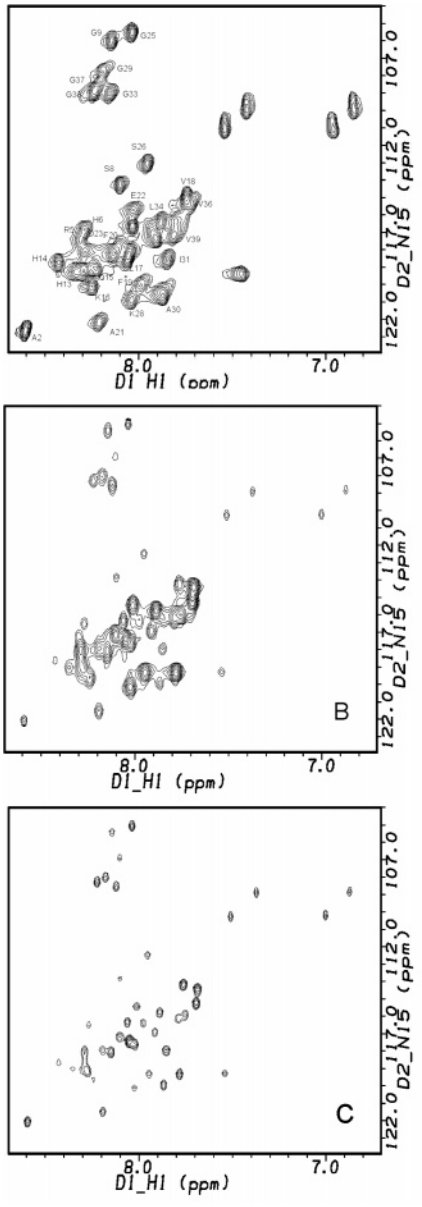

FIGURE 4: HSQC spectra acquired with *U*-^{15}N Aβ_{1-40} fibrils dissolved in DMSO/DCA. (A) Fully protonated dissolved fibrils. (B) Spectrum representing data acquisition started 14 min after dissolving the fibrils in DMSO/DCA. (C) Same sample in B after 3 h. All spectra were processed with identical parameters and shown with the same contour levels.

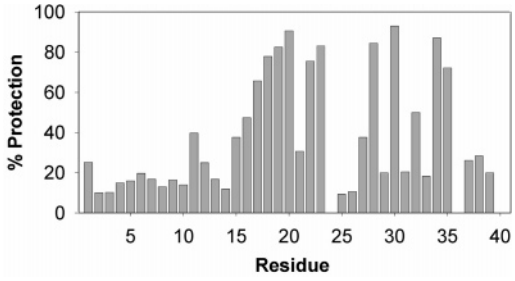

FIGURE 5: Bar plot showing the residue-specific protection of the backbone amides of Aβ_{1-40} fibrils. No information is available on residues 24, 26, and 40, which have ambiguous resonance assignments. Unprotected residues appear to have ~10% protection, which is due to the final H_2O/D_2O composition of the solvent.

data is the very low protection observed in residues G25 and G26 in the central part of the sequence. A particularly

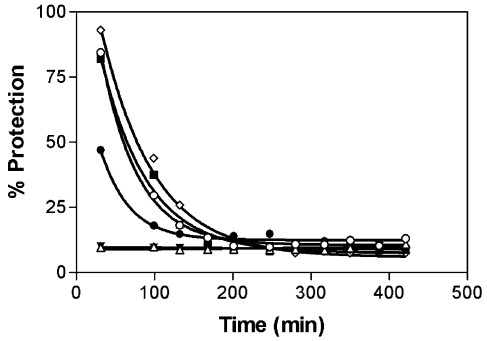

FIGURE 6: Exchange of the residual backbone protons of Aβ_{1-40} after the dissolution of fibrils in deuterated DMSO/DCA mixture. Curves represent fitted lines of the measured peak volumes to a single-exponential decay with plateau (◇) A30, (○) K28, (■) F19, and (●) K16. Two unprotected residues are also shown (▼) A2 and (△) G25.

surprising aspect of the data is the protection pattern of the residues between 28 and 35, which exhibit an almost perfect pattern of alternating exposure and protection, with K28, A30, I32, L34, and M35 being highly protected, while the intervening residues are much less protected.

The ^{1}H-^{15}N HSQC spectra acquired after the dissolution of fibrils showed that strong cross-peaks also lost their intensity as a function of time and, after ~120 min, all cross-peaks reach the same basal intensity (Figure 6), which represents the equilibrium level of residual H/D ratio present in the solvent. The time dependence of this artifactual forward exchange plotted for three types of protons, fully protected (>80%), somewhat protected (~50%), and unprotected (<20%), is shown in Figure 6. The curves observed with protected protons (full or partial) with well-resolved peaks can be fitted to a single-exponential decay with plateau. The rate constants are within a factor of 2, regardless of the level of protection in the fibril (however, it is clearly not possible to monitor a significant amplitude of forward exchange in the amide protons that were not protected). To determine these artifactual exchange rates, the initial 14 min delay was added to the midpoints of spectral data acquisition to estimate the time points. This is done to account for the differential effects of saturation transfer on the intensity and line width of signals during the data acquisition because each HSQC spectrum was acquired in 33.5 min, which represents more than 25% of the entire exchange period. These data suggest that the residues of the monomer obtained by fibril dissolution are exposed to the solvent approximately equally and that therefore the strong cross-peaks in the initial ^{1}H-^{15}N HSQC spectra are not due to a rapid back exchange in the dissolved fibril but rather represent the protons that are protected from exchange when fibrils are incubated in D_2O. Also, separate experiments performed with the Aβ monomer showed that all or most of the protons of the peptide are readily exchanged upon treatment with D_2O under similar conditions (Figure S3 in the Supporting Information). This observation lends further support to our conclusions that data observed in HSQC spectra represent H/D exchange characteristics of the fibril.

DISCUSSION

The exchange data shown in Figure 5 are broadly consistent with previous models of the Aβ fibril derived from other biophysical measurements. In particular, the relatively free exchange within the fibril of the amide protons from residues 1−14 is consistent with a variety of experiments suggesting that this portion of the peptide is not involved in the hydrogen-bonded core of the fibril (*5*, *10*−*12*). In addition, the new H/D exchange NMR data are consistent with two expanses of the protective structure, one centered in residues 15−23 and the other centered at residues 28−35, consistent with the Aβ peptide folding back on itself to form an enclosed structure exhibiting at least two elements of β structure. The existence of the β-extended structure around residues 17−20 and 30−35 is another common feature of Aβ amyloid fibril models (*10*−*12*). The NMR-based H/D data described here are also in good overall agreement with H/D exchange data on the same fibrils as evaluated by mass spectrometry. When previously obtained (*6*) HX-MS kinetics data on fibrils of Aβ_{1-40} are corrected for back exchange (*33*), one obtains the kinetics shown in Figure 3 consistent with 54% (21:39) of the backbone amide protons being protected in the first 25 h of exchange time. If, in Figure 5, any residue protected at a minimum level of 30% is counted as one protected amide proton and if two of the three unresolved amide protons are also protected (as expected from their sequence context), then the NMR-based H/D exchange experiment yields 46% (18:39) protection. While the results of the two approaches (conducted within the same research consortium on identical fibrils) do not agree perfectly, both are consistent with approximately 50% of the backbone amide groups being excluded from the hydrogen-bonded structure, as predicted by current models of the Aβ fibril.

One area that is clearly different in various Aβ_{1-40} models is the C terminus. Solid-state NMR data suggests that the C-terminal residues of Aβ_{1-40} lie in the β structure in the fibril (*10*). However, proline scanning/stability analysis shows that fibril stability is not affected by proline replacements in the C terminus, suggesting a more flexible structure in that region. The H/D NMR data reported here show that the backbone amide protons of residues 37−39 are essentially as unprotected from exchange as are the amide protons in the flexible N terminus of Aβ. This is also consistent with recent H/D data analyzed by protease fragmentation and MS that also clearly shows the Aβ_{1-40} C terminus to be unprotected in the amyloid fibril (Kheterpal, I., Chen, M., Cook, K., and Wetzel, R., manuscript in preparation). The source of this discrepancy with the solid-state NMR data is not evident but may be due to different fibril preparations. It is also possible that C-terminal residues may exhibit extended chain conformation and chain−chain proximity without actually forming stable hydrogen bonds, perhaps because of structural constraints required for amyloid formation. This lack of involvement of the C terminus of Aβ_{1-40} fibrils in stable hydrogen bonding is not in conflict with the well-documented importance of the C terminus in disease-related aggregation (*34*) and toxicity (*35*). First, the toxic aggregate may not be an amyloid fibril (*36*, *37*), and the structural role of the C terminus in alternative aggregated structures of Aβ may be different from that in the fibril [However, recent studies suggest that the C terminus of the Aβ_{1-40} peptide is also not in a rigid structure in the protofibril (Williams, A., Sega, M., Kheterpal, I., Chen, M., Cook, K., and Wetzel, R., manuscript submitted)]. It is also possible

that the role of the C terminus in fibril formation may be different in the more toxic 1−42 form of Aβ.

Different techniques also indicate different roles for residues in the 22−30 region of Aβ_{1-40}. Scanning proline mutagenesis and stability analysis suggested turns centered at residues 22, 23 and 29, 30, with residues 24−28 in a rigid structure presumed to be a β sheet (*12*). Solid-state NMR experiments, however, have been interpreted to indicate that the first element of the β sheet in the fibril includes residues 22 and 23, with a turn occupying residues 24−28 (*10*). The H/D NMR data shown in Figure 5 is more supportive of the latter model, although it remains possible that residues 22 and 23 might occupy a bend that is sensitive to Pro replacement but not sufficiently deformed to prevent hydrogen bonding to adjacent strands. It is also possible that the destabilization of fibril structure by proline substitution in this Aβ segment might also reflect the existence of rigid, proline-incompatible geometries other than the β-extended chain.

The source of the unusual and unprecedented alternating pattern of protection and exposure seen in the region 28−34 is difficult to explain. All fibril models posit that this segment exists predominantly in an independent β sheet within the amyloid fibril, packed against the sheet formed by residues 17−20. This requires all of the backbone amide protons to be involved in hydrogen bonds with neighboring strands in the sheet. The alternating pattern shown in Figure 5, if confirmed by future experiments, will require a radical rethinking of the role of this segment in the amyloid structure. One possible interpretation is that the 31−36 region is involved in a β sheet that is surface-exposed, allowing the sheet to breath and hence undergo more facile exchange; it remains unclear why this exchange would be alternating rather than global. However, one implication of this interpretation is that the dominant β-sheet interface between Aβ peptides within the fibril would then most likely involve the 15−21 segment, rather than the 30−37 segment. Involvement of the 15−21 segment in β-sheet-packing interactions in the fibril both within the folded monomer and between folded monomers might help explain the dominant role of this sequence element in Aβ amyloid fibril formation and stability, as indicated by a wide variety of published experiments (*12*, *38*).

While this paper was under review, a new report was published (*39*) describing solid-state NMR analysis of Aβ-(1−40) fibrils grown without agitation, conditions presumably analogous to those used in the analysis described here. Some new structural details from this latest solid-state NMR analysis are in agreement with the H/D NMR protection data, in particular the lack of evidence for hydrogen bonding in residues 29, 37, and 38, and the positive evidence for the non-β-sheet structure in residues 25 and 33. Discrepancies persist, as well, including the structural roles of residues 10−14 and 23.

The studies presented here represent the first example of H/D NMR experiments on amyloid fibrils where there is substantial independent data on the fibril structure from other techniques. Overall, the comparison of these data with that of other methods is encouraging and suggests that future experiments by a variety of techniques should continue to solidify our knowledge about the amyloid fibril structure. Further knowledge will be gained from experiments aimed at determining the orientations and contacts of individual amino acid side chains within the packed fibril core (*40*) as well as outside the core, the role of the flexible, extruded portions of polypeptide chain in the fibril structure, and the basis of protofilament packing.

ACKNOWLEDGMENT

The authors thank Dr. John R. Dunlap of the Electron Microscopy Program at the University of Tennessee—Knoxville for the acquisition of the electron micrographs of the batches of fibrils used in this study.

SUPPORTING INFORMATION AVAILABLE

Table S1, the ^{1}H and ^{15}N resonance assignments of Aβ_{1-40} fibrils dissolved in DMSO/DCA; electron micrographs of the fibrils formed by WT and ^{15}N-enriched Aβ_{1-40} monomers, shown in Figure S1; the entire ^{1}H-^{15}N HSQC spectrum with all of the cross-peaks labeled, shown in Figure S2; Figures S3 and S4, 1D ^{1}H NMR spectra obtained with D_2O-treated Aβ_{1-40} monomer and Aβ_{1-40} fibrils. This material is available free of charge via the Internet at http://pubs.acs.org.

REFERENCES

1. Turner, G. C., and Varshavsky, A. (2000) Detecting and measuring cotranslational protein degradation *in vivo*, *Science 289*, 2117−2120.
2. Martin, J. B. (1999) Molecular basis of the neurodegenerative disorders [published erratum appears in (1999) *N. Engl. J. Med. 341*, 1407], *N. Engl. J. Med. 340*, 1970−1980.
3. Tycko, R. (2004) Progress towards a molecular-level structural understanding of amyloid fibrils, *Curr. Opin. Struct. Biol. 14*, 96−103.
4. Sunde, M., Serpell, L. C., Bartlam, M., Fraser, P. E., Pepys, M. B., and Blake, C. C. F. (1997) Common core structure of amyloid fibrils by synchrotron X-ray diffraction, *J. Mol. Biol. 273*, 729−739.
5. Kheterpal, I., Williams, A., Murphy, C., Bledsoe, B., and Wetzel, R. (2001) Structural features of the Aβ amyloid fibril elucidated by limited proteolysis, *Biochemistry 40*, 11757−11767.
6. Kheterpal, I., Zhou, S., Cook, K. D., and Wetzel, R. (2000) Aβ amyloid fibrils possess a core structure highly resistant to hydrogen exchange, *Proc. Natl. Acad. Sci. U.S.A. 97*, 13597−13601.
7. Kheterpal, I., Lashuel, H. A., Hartley, D. M., Walz, T., Lansbury, P. T., and Wetzel, R. (2003) Aβ protofibrils possess a stable core structure resistant to hydrogen exchange, *Biochemistry 42*, 14092−14098.
8. Petkova, A. T., Leapman, R. D., Yau, W. M., and Tycko, R. (2004) Structural investigations of Alzheimer's β-amyloid fibrils by solid-state NMR, *Biophys. J. 86*, 506A.
9. Benzinger, T. L., Gregory, D. M., Burkoth, T. S., Miller-Auer, H., Lynn, D. G., Botto, R. E., and Meredith, S. C. (1998) Propagating structure of Alzheimer's β-amyloid(10−35) is parallel β-sheet with residues in exact register, *Proc. Natl. Acad. Sci. U.S.A. 95*, 13407−13412.
10. Antzutkin, O. N., Leapman, R. D., Balbach, J. J., and Tycko, R. (2002) Supramolecular structural constraints on Alzheimer's β-amyloid fibrils from electron microscopy and solid-state nuclear magnetic resonance, *Biochemistry 41*, 15436−15450.
11. Torok, M., Milton, S., Kayed, R., Wu, P., McIntire, T., Glabe, C. G., and Langen, R. (2002) Structural and dynamic features of Alzheimer's A β peptide in amyloid fibrils studied by site-directed spin labeling, *J. Biol. Chem. 277*, 40810−40815.
12. Williams, A. D., Portelius, E., Kheterpal, I., Guo, J. T., Cook, K. D., Xu, Y., and Wetzel, R. (2004) Mapping Aβ amyloid fibril secondary structure using scanning proline mutagenesis, *J. Mol. Biol. 335*, 833−842.
13. Wang, S. S. S., Tobler, S. A., Good, T. A., and Fernandez, E. J. (2003) Hydrogen exchange-mass spectrometry analysis of β-amyloid peptide structure, *Biochemistry 42*, 9507−9514.

14. Milne, J. S., Mayne, L., Roder, H., Wand, A. J., and Englander, S. W. (1998) Determinants of protein hydrogen exchange studied in equine cytochrome *c*, *Protein Sci. 7*, 739−745.
15. Englander, S. W., Sosnick, T. R., Englander, J. J., and Mayne, L. (1996) Mechanisms and uses of hydrogen exchange, *Curr. Opin. Struct. Biol. 6*, 18−23.
16. Hoshino, M., Katou, H., Hagihara, Y., Hasegawa, K., Naiki, H., and Goto, Y. (2002) Mapping the core of the β(2)-microglobulin amyloid fibril by H/D exchange, *Nat. Struct. Biol. 9*, 332−336.
17. Ippel, J. H., Olofsson, A., Schleucher, J., Lundgren, E., and Wijmenga, S. S. (2002) Probing solvent accessibility of amyloid fibrils by solution NMR spectroscopy, *Proc. Natl. Acad. Sci. U.S.A. 99*, 8648−8653.
18. Kuwata, K., Matumoto, T., Cheng, H., Nagayama, K., James Thomas, L., and Roder, H. (2003) NMR-detected hydrogen exchange and molecular dynamics simulations provide structural insight into fibril formation of prion protein fragment 106−126, *Proc. Natl. Acad. Sci. U.S.A. 100*, 14790−14795.
19. Olofsson, A., Ippel, J. H., Wijmenga, S. S., Lundgren, E., and Ohman, A. (2004) Probing solvent accessibility of transthyretin amyloid by solution NMR spectroscopy, *J. Biol. Chem. 279*, 5699−5707.
20. Mishra, R., Whittemore, N. A., Kheterpal, I., Wetzel, R., and Serpersu, E. (2004) in *National Meeting of the Protein Society*, San Diego, CA.
21. States, D. J., Haberkorn, R. A., and Ruben, D. J. (1982) A two-dimensional nuclear Overhauser experiment with pure absorption phase in 4 quadrants, *J. Magn. Reson. 48*, 286−292.
22. Jeener, J., Meier, B. H., Bachmann, P., and Ernst, R. R. (1979) Investigation of exchange processes by two-dimensional NMR spectroscopy, *J. Chem. Phys. 71*, 4546−4553.
23. Shaka, A. J., Lee, C. J., and Pines, A. (1988) Iterative schemes for bilinear operators−Application to spin decoupling, *J. Magn. Reson. 77*, 274−293.
24. Kay, L. E., Keifer, P., and Saarinen, T. (1992) Pure absorption gradient enhanced heteronuclear single quantum correlation spectroscopy with improved sensitivity, *J. Am. Chem. Soc. 114*, 10663−10665.
25. Wishart, D. S., Bigam, C. G., Yao, J., Abildgaard, F., Dyson, H. J., Oldfield, E., Markley, J. L., and Sykes, B. D. (1995) ^{1}H, ^{13}C, and ^{15}N chemical-shift referencing in biomolecular NMR, *J. Biomol. NMR 6*, 135−140.
26. Bax, A., Vuister, G. W., Grzesiek, S., Delaglio, F., Wang, A. C., Tschudin, R., and Zhu, G. (1994) Measurement of homonuclear and heteronuclear J-couplings from quantitative J-correlation, *Methods Enzymol. 239*, 79−105.
27. Yamaguchi, K. I., Katou, H., Hoshino, M., Hasegawa, K., Naiki, H., and Goto, Y. (2004) Core and heterogeneity of β(2)-microglobulin amyloid fibrils as revealed by H/D exchange, *J. Mol. Biol. 338*, 559−571.
28. Hirota-Nakaoka, N., Hasegawa, K., Naiki, H., and Goto, Y. (2003) Dissolution of β(2)-microglobulin amyloid fibrils by dimethylsulfoxide, *J. Biochem. 134*, 159−164.
29. Wüthrich, K. (1986) *NMR of Proteins and Nucleic Acids*, John Wiley and Sons, New York.
30. Redfield, C. (1993) in *NMR of Macromolecules, A Practical Approach* (Roberts, G. C. K., Ed.) pp 71−101, IRL Press, Oxford, U.K.
31. Mikros, E., Benaki, D., Humpfer, E., Spraul, M., Loukas, S., Stassinopoulou, C. I., and Pelecanou, M. (2001) High-resolution NMR spectroscopy of the β-amyloid(1−28) fibril typical for Alzheimer's disease, *Angew. Chem. 40*, 3603−3605.
32. Coles, M., Bicknell, W., Watson, A. A., Fairlie, D. P., and Craik, D. J. (1998) Solution structure of amyloidβ peptide(1−40) in a water−micelle environment. Is the membrane-spanning domain where we think it is? *Biochemistry 37*, 11064−11077.
33. Kheterpal, I., Wetzel, R., Cook, K. (2003) Enhanced correction methods for hydrogen exchange-mass spectrometry studies of amyloid fibrils, *Protein Sci.* 12, 635−643.
34. Jarrett, J. T., Berger, E. P., and Lansbury, P. T., Jr. (1993) The carboxy terminus of the β-amyloid protein is critical for the seeding of amyloid formation: Implications for the pathogenesis of Alzheimer's disease, *Biochemistry 32*, 4693−4697.
35. Selkoe, D. J. (1999) Translating cell biology into therapeutic advances in Alzheimer's disease, *Nature 399*, A23−A31.
36. Kirkitadze, M. D., Bitan, G., and Teplow, D. B. (2002) Paradigm shifts in Alzheimer's disease and other neurodegenerative disorders: The emerging role of oligomeric assemblies, *J. Neurosci. Res. 69*, 567−577.
37. Caughey, B., and Lansbury, P. T. (2003) Protofibrils, pores, fibrils, and neurodegeneration: Separating the responsible protein aggregates from the innocent bystanders, *Annu. Rev. Neurosci. 26*, 267−298.
38. Esler, W. P., Stimson, E. R., Ghilardi, J. R., Lu, Y. A., Felix, A. M., Vinters, H. V., Mantyh, P. W., Lee, J. P., Maggio, J. E. (1996) Point substitution in the central hydrophobic cluster of a human β-amyloid congener disrupts peptide folding and abolishes plaque competence, *Biochemistry* 35, 13914−13921.
39. Petkova, A. T., Leapman, R. D., Guo, Z., Yau, W.-M., Mattson, M. P., Tycko, R. (2005) Self-propagating, molecular-level polymorphism in Alzheimer's β-amyloid fibrils, *Science* 307, 262−265.
40. Shivaprasad, S. and Wetzel, R. (2004) An intersheet packing interaction in Aβ fibrils mapped by disulfide crosslinking, *Biochemistry* 43, 15310−15317.

BI048292U